ARR No. 3H26

NATIONAL ADVISORY COMMITTEE FOR AERONAUTICS

WARTIME REPORT

ORIGINALLY ISSUED

August 1943 as
Advance Restricted Report 3H26

AN INVESTIGATION OF AIRCRAFT HEATERS

XIII - PERFORMANCE OF CORRUGATED AND NONCORRUGATED FLUTED TYPE EXHAUST GAS-AIR HEAT EXCHANGERS

By L. M. K. Boelter, A. G. Guibert,
M. A. Miller, and E. H. Morrin
University of California

NACA

WASHINGTON

NATIONAL ADVISORY COMMITTEE FOR AERONAUTICS

ADVANCE RESTRICTED REPORT

AN INVESTIGATION OF AIRCRAFT HEATERS XIII - PERFORMANCE OF CORRUGATED AND NONCORRUGATED FLUTED TYPE EXHAUST GAS-AIR HEAT EXCHANGERS

By L. M. K. Boelter, A. G. Guibert, M. A. Miller, and E. H. Morrin

SUMMARY

Thermal and static pressure-drop performance data on three fluted-type heat exchangers are presented. Two of the heaters utilized corrugated surfaces along the fluid passages and the third one was constructed with non-corrugated surfaces. In these tests all heaters were fitted with the same air shroud. Previously reported data taken on the latter heater, but with a different air shroud, are compared with the current data.

Exhaust-gas rates from 3500 pounds per hour to 6600 pounds per hour and ventilating-air rates from 1500 pounds per hour to 4700 pounds per hour were used. Pressure-drop measurements were made across the exhaust-gas and ventilating-air sides of the exchanger under both isothermal and nonisothermal conditions.

The measured thermal outputs and static pressure drops are compared with predicted magnitudes.

INTRODUCTION

Two corrugated fluted type heaters (copper and stainless steel) and another heater of the same type but with plain, noncorrugated passages (stainless steel) were tested in the large test stand of the Mechanical Engineering Laboratories of the University of California. (See description of this test stand in reference 1.)

These heaters are designed for use in the exhaust-gas streams of aircraft engines for cabin, wing, and tail-surface heating systems.

The following data were obtained:

1. Weight rates of exhaust-gas and ventilating air through the two sides of the heat exchanger

2. Temperatures of ventilating air and exhaust gas at entrance and exit of the heater

3. Temperatures of the heater surfaces

4. Static pressure-drop measurements on the exhaust-gas and ventilating-air sides of the heater under both isothermal and nonisothermal flow conditions.

This report is one of a series of advance restricted reports that describe research being conducted on aircraft heat exchangers at the University of California under the sponsorship and with the financial assistance of the National Advisory Committee for Aeronautics.

DESCRIPTION OF THE HEATERS AND OF THE TESTING PROCEDURE

The fluted-type heaters tested were all prime-surface parallel-flow units. The fluted passages, constructed of either copper or stainless steel, are tapered at each end of the heater.

The corrugated fluted type heaters consist of 34 alternate ventilating-air and exhaust-gas passages in the case of the copper heater and 52 alternate ventilating-air and exhaust-gas passages in the case of the stainless-steel heater. (See fig. 16.) These passages are formed from sheets of corrugated metal so that the distance between the walls is constant along the passage, that is, the passage is sinuous in character. The corrugations are spaced $\frac{3}{4}$ inch apart and are arranged perpendicularly to the direction of flow of the fluids.

The heater, constructed of noncorrugated stainless steel and containing 32 fluid passages, was also tested previously using a different air shroud. The results of the data obtained at that time were reported in reference 1. The air shroud used in the tests reported here differs from the previous one only in the configuration of the inlet air ducts.

Diagrams and photographs of these heaters are shown in figures 1 to 4 and 16.

The weight rates of exhaust gas and ventilating air were obtained by means of calibrated square-edge orifices.

The exhaust-gas temperatures were measured at the inlet and outlet of the heater by means of shielded, traversing thermocouples. Unshielded, traversing thermocouples were used for the ventilating-air temperature measurements.

Temperatures of the heater surfaces were measured at six points by means of thermocouples. (See fig. 16.) Three of the thermocouples were located on the ventilating-air side of the heater shell, near the exhaust-gas inlet - the other three thermocouples being similarly located near the exhaust-gas outlet. The three thermocouples in each group are spaced at approximately equal intervals around the circumference.

The arithmetic average of the readings of the three thermocouples located near the exhaust-gas inlet is designated as t_1, whereas the arithmetic average of the readings of the three thermocouples located near the downstream end of the heater is designated as t_2. (See figs. 1 and 16 and tables I and II.)

Static pressure-drop measurements were made across the ventilating-air and exhaust-gas sides of the heater. Two taps, 180° apart, were installed at each pressure-measuring station.

NOTATION

A area of heat transfer, ft^2

A_a total cross-sectional area of the passages on the ventilating-air side of the heater, ft^2

A_g total cross-sectional area of the passage on the exhaust-gas side of the heater, ft^2

c_{p_a} heat capacity of air at constant pressure, Btu/lb ^oF

c_{p_g} heat capacity of exhaust gas at constant pressure, Btu/lb ^oF

D hydraulic diameter, ft

D_a hydraulic diameter on ventilating-air side, ft

D_g hydraulic diameter on exhaust-gas side, ft

f_c unit thermal convective conductance (av. with length), Btu/hr ft^2 ^oF

f_{c_a} unit thermal convective conductance for the ventilating air (av. with length), Btu/hr ft^2 ^oF

f_{c_g} unit thermal convective conductance for the exhaust gas (av. with length), Btu/hr ft^2 ^oF

g gravitational force per unit of mass, lb/(lb sec^2/ft)

G weight rate per unit of area, lb/hr ft^2

G_a weight rate per unit of area for ventilating air, lb/hr ft^2

G_g weight rate per unit of area for exhaust gas, lb/hr ft^2

K isothermal pressure drop factor defined by the equation $\frac{\Delta P}{\gamma} = K \frac{u_m^2}{2g}$

l significant dimension in equations for f_c along flat plate, ft

L length of heat transfer surface, ft

P heat transfer perimeter, ft

q_a measured rate of enthalpy change of ventilating air, Btu/hr or k Btu/hr (= 1000 Btu/hr)*

q_g measured rate of enthalpy change of exhaust gas, Btu/hr or k Btu/hr (= 1000 Btu/hr)*

* kBtu designates kilo btu.

t_1 arithmetic average of three surface temperature measurements taken near the exhaust-gas inlet, °F

t_2 arithmetic average of three surface temperature measurements taken near the exhaust-gas outlet, °F

T_a arithmetic average mixed-mean absolute temperature of ventilating air $= \frac{T_{a_1} + T_{a_2}}{2} + 460$, °R

T_{av} arithmetic average mixed-mean absolute temperature of fluid $= \frac{T_1 + T_2}{2}$, °R

T_g arithmetic average mixed-mean absolute temperature of exhaust gas $= \frac{T_{g_1} + T_{g_2}}{2} + 460$, °R

T_1 mixed-mean absolute temperature of fluid at entrance section (point 1), °R

T_2 mixed-mean absolute temperature of fluid at exit section (point 2), °R

T_{iso} mixed-mean absolute temperature of fluid for isothermal pressure drop tests, °R

u_m mean velocity of fluid at minimum cross-sectional area of fluid passages, ft/sec

U over-all unit thermal conductance, Btu/hr ft^2 °F

(UA) over-all thermal conductance, Btu/hr °F

W weight rate of fluid, lb/hr

W_a weight rate of air, lb/hr

W_g weight rate of exhaust gas, lb/hr

γ_1 weight density of fluid at entrance to heating section (point 1), lb/ft^3

ΔP static pressure drop, lb/ft^2

ΔP_a total static pressure drop on ventilating-air side, lb/ft^2

$\Delta P'_a$ total static pressure drop on ventilating-air side, inches H_2O

ΔP_g total static pressure drop on exhaust-gas side, lb/ft^2

$\Delta P'_g$ total static pressure drop on exhaust-gas side, inches H_2O

ΔP_{duct} isothermal static pressure drop along inlet and outlet ducts of the air shroud, lb/ft^2

ΔP_{htr} isothermal static pressure drop along the heater passages only, lb/ft^2

ΔP_{iso} total isothermal static pressure drop along heater and ducts at temperature T_{iso}, lb/ft^2

ζ_{iso} isothermal friction factor defined by the equation, $\frac{\Delta P}{\gamma} = \zeta \frac{L}{D} \frac{u_m^2}{2g}$

Δt_m logarithmic mean temperature difference defined by equation (4), ^oF

ΔT_a difference between mixed-mean temperature of ventilating air at sections defined by points 1 and 2 = $(T_{a_2} - T_{a_1})$, ^oF

ΔT_g difference between mixed-mean temperatures of exhaust gas at sections defined by points 1 and 2 = $(T_{g_1} - T_{g_2})$, ^oF

μ viscosity of fluid, $lb \cdot sec/ft^2$

T_{a_1} mixed-mean temperature of ventilating air at entrance section (point 1), ^oF

T_{a_2} mixed-mean temperature of ventilating air at exit section, (point 2), ^oF

T_{g_1} mixed-mean temperature of exhaust gas at entrance section (point 1), ^oF

T_{g_2} mixed-mean temperature of exhaust gas at exit section (point 2), ^oF

Re Reynolds number = $GD/3600 \mu g$

METHOD OF ANALYSIS

Heat Transfer

The thermal output of the heaters was determined by the enthalpy change of the ventilating air:

$$q_a = W_a \, c_{p_a} \, (T_{a_2} - T_{a_1}) \tag{1}$$

in which c_{p_a} was evaluated at the arithmetic average ventilating-air temperature as a good approximation. A plot of q_a against W_a at constant values of the exhaust-gas rate (W_g) is shown in figures 6 and 10.

On the exhaust-gas side of the heater:

$$q_g = W_g \, c_{p_g} \, (T_{g_1} - T_{g_2}) \tag{2}$$

where c_{p_g} was evaluated for air at the arithmetic average exhaust-gas temperature.

The over-all thermal conductance UA was evaluated from the expression

$$q_a = (UA) \, \Delta t_{lm} \tag{3}$$

where Δt_{lm} is the log-mean temperature difference defined by the equation

$$\Delta t_{lm} = \frac{(T_{g_1} - T_{a_1}) - (T_{g_2} - T_{a_2})}{\ln \dfrac{(T_{g_1} - T_{a_1})}{(T_{g_2} - T_{a_2})}} \tag{4}$$

The variations of UA with W_a and W_g are shown graphically in figures 7 and 11. The termal output of the heater for values of Δt_{lm} other than those used here

may be predicted by determining UA at the actual weight rates from figures 7 and 11 and using these magnitudes in equation (3)*

Predictions of the magnitudes of the over-all thermal conductance (UA) were attempted. The expression

$$UA = \frac{1}{\left(\frac{1}{f_c A}\right)_a + \left(\frac{1}{f_c A}\right)_g} \qquad (5)$$

was used (reference 2, equation (4)).

The heat transfer area (A) is based upon the heat transfer perimeter measured at the center of the fully fluted section of the heater and upon a length which consists of that of the fully fluted center section plus one half the length of each of the tapered ends. For example, in the case of the stainless steel noncorrugated heater (see data on fig. 16):

Length of fully fluted section, 0.917 ft

Length of each tapered end, 0.354 ft

Heat transfer perimeter at section A-A, 5.66 ft = P

The equivalent length of heat transfer surface is then

$$L = \frac{0.354}{2} + 0.917 + \frac{0.354}{2} = 1.27 \text{ ft}$$

Heat transfer area, $A = P\,L = 5.66 \times 1.27 = 7.19 \text{ ft}^2$

The choice of this length is somewhat arbitrary but it probably yields a conservative value of the over-all thermal conductance (UA).

The unit thermal conductances f_{c_a} and f_{c_g} on the ventilating-air and exhaust-gas sides, respectively, are evaluated from the following equations:

---

*See alternate method for computing heater output for the case when only the initial temperatures of the air and gas are known (reference 12).

(a) For the stainless steel noncorrugated fluted heater

$$f_{c_a} = 5.56 \times 10^{-4} T_a^{0.888} \frac{G_a^{0.8}}{D_a^{0.2}} \qquad (6)$$

and

$$f_{c_g} = 5.56 \times 10^{-4} T_g^{0.888} \frac{G_g^{0.8}}{D_g^{0.2}} \qquad (7)$$

in which D is the hydraulic diameter. These equations are valid for the calculation of the unit thermal conductance (f_c) for forced convection in smooth, straight ducts in which the fluid and heat-flow mechanisms correspond to those in the turbulent regime.* The values of the thermal resistances $(1/f_cA)_a$ and $(1/f_cA)_g$ can also be obtained by use of chart B of references 1 and 2. (See reference 2 for the derivation of equations (6) and (7).)

(b) For the copper and stainless steel corrugated fluted heaters:

$$f_{c_a} = 9.36 \times 10^{-4} T_a \frac{G_a^{0.8}}{l^{0.2}} \qquad (8)$$

and

$$f_{c_g} = 9.36 \times 10^{-4} T_g \frac{G_g^{0.8}}{l^{0.2}} \qquad (9)$$

These expressions are based on data for heat transfer by forced convection over flat plates of length l, measured in the direction of the flow of the fluid. Equations (8) and (9) are valid only in the region downstream from the point where the flow in the retarded layer along the plate has changed from laminar to turbulent flow. The flow in

*See Discussion of this report for comment on effect of diameter to length ratio for ducts or channels.

the retarded layer near the leading edge of the plate is usually laminar, in which case the unit thermal conductance (f_c) is a function of the 0.5 power of G and of the -0.5 power of l.

The use of these equations, based on flat-plate heat-transfer data long the corrugated passages of the heaters tested, implies that a retarded layer is initiated at the crest of each corrugation because the value of the significant dimension l was taken to be $\frac{3}{4}$ inch, the distance between successive crests of the corrugated passages.

Sample Calculation of (UA)

(For run 49 on noncorrugated fluted type heater. Data from table I and fig. 15.)

(a) Computation of $f_{c_a} = 5.56 \times 10^{-4} T_a^{0.296} \times \frac{G_a^{0.8}}{D_a^{0.2}}$

$$T_a = \frac{98^\circ + 252^\circ}{2} + 460^\circ = 635^\circ \text{ R}$$

$$G_a = \frac{W_a}{A_a} = \frac{4550 \text{ lb/hr}}{0.112 \text{ ft}^2} = 40{,}600 \text{ lb/hr ft}^2$$

$$D_a = 4 \times \frac{A_a}{\text{wetted perimeter}} = 4 \times \frac{0.112}{7.60} = 0.0589 \text{ ft}$$

$$f_{c_a} = 5.56 \times 10^{-4} (635)^{0.296} \times \frac{(40{,}600)^{0.8}}{(0.0589)^{0.2}}$$

$$= 32.0 \text{ Btu/hr ft}^2 \text{ }^\circ\text{F}$$

(b) Computation of $f_{c_g} = 5.56 \times 10^{-4} T_g^{0.296} \times \frac{G_g^{0.8}}{D_g^{0.2}}$

$$T_g = \frac{1420^\circ + 1372^\circ}{2} + 460^\circ = 1850^\circ \text{ R}$$

$$G_g = \frac{6670 \text{ lb/hr}}{0.194 \text{ ft}^2} = 34{,}400 \text{ lb/hr ft}^2$$

$$D_g = 4 \times \frac{A_g}{\text{wetted perimeter}} = 4 \times \frac{0.194}{7.68} = 0.101 \text{ ft}$$

$$f_{c_g} = 5.56 \times 10^{-4} \, (1850)^{0.888} \times \frac{(34{,}400)^{0.8}}{(0.101)^{0.8}}$$

$$= 34.8 \text{ Btu/hr ft}^2 \, ^\circ\text{F}$$

(c) Computation of $UA = \dfrac{1}{\dfrac{1}{(f_c A)_a} \dfrac{1}{(f_c A)_g}}$

$$A = 7.19 \text{ ft}^2$$

$$UA = \frac{1}{\dfrac{1}{32.0 \times 7.19} + \dfrac{1}{34.8 \times 7.19}} \qquad \frac{1}{0.00435 + 0.00400}$$

$$= \frac{1}{0.00835}$$

$$UA = 120 \text{ Btu/hr } ^\circ\text{F}$$

The value of UA obtained from the laboratory measurements of q_a was (see fig. 7):

$$UA = \frac{q_a}{\Delta t_{lm}} = \frac{170{,}000 \text{ Btu/hr}}{1130^\circ\text{F}} = 150 \text{ Btu/hr } ^\circ\text{F}$$

Percent deviation of the predicted magnitude from the measured magnitude was −20 percent.

Pressure Drop

Isothermal Pressure Drop.— Because of the complex curvature of the inlet and outlet ventilating-air ducts, the isothermal pressure drop through these ducts could not be predicted satisfactorily. However, due to the fact that these inlet and outlet ducts were used with both the plain and corrugated fluted type heaters, the influence of the corrugations of the heater metal upon the pressure drop along the fluid passages could be determined from the total measured pressure drop along both the heater and air ducts.

The isothermal pressure drops through the corrugated-fluted passages on the air side of the heater were calculated in the following manner:

(a) The pressure drop along the air passages of the plain, uncorrugated fluted passages was calculated by means of the equation

$$\frac{\Delta P_{htr}}{\gamma} = \zeta_{iso} \frac{L}{D} \frac{u_m^2}{2g} \qquad (10)$$

where ζ_{iso} was taken as the friction factor for commercial tubes.

(b) This pressure drop was subtracted from the total drop in pressure across the heater (ΔP_{iso}) to obtain the losses in the inlet and outlet ducts

$$\Delta P_{duct} = \Delta P_{iso} - \Delta P_{htr} \qquad (11)$$

(c) Since the same inlet and outlet ducts were also used on the corrugated fluted heaters, the duct losses calculated from equation (11) using the measurements on the non-

corrugated fluted unit were subtracted from the total measured pressure drop across the corrugated fluted heater, yielding approximately* the pressure drop in the corrugated air passages. Thus equation (11) was used to compute the pressure drop along the air passages of the corrugated fluted heaters.

(d) The friction factor was then obtained from equation (10).

In this manner the friction factor ζ_{iso} for the corrugated surfaces was computed and is tabulated in tables III and IV.

In order to utilize existing data for fittings, and so forth, for the estimation of the pressure drop in the air ducts, equation (10) is used in the form

$$\frac{\Delta P}{\gamma} = K \frac{u_m^2}{2g} \qquad (12)$$

In the case of the frictional pressure drop in straight ducts,

$$K \equiv \left(\zeta_{iso} \frac{L}{D} \right) \qquad (13)$$

By evaluating the magnitude of K in equation (12) for the complex inlet and outlet air ducts, it was found that the pressure drop through these ducts could be calculated approximately by using a value of K = 1.0 to 1.5, corresponding to sharp 90° bends. (See references 4 to 8.) Hence, the function of these ducts in conducting the ventilating-air through the heater passages is approximately that of a 90° bend.

On the exhaust-gas side of the heaters, the isothermal friction factor ζ_{iso} was calculated by means of equation (10). In this case, $\Delta P_{iso} = \Delta P_{htr}$, because the pressure drop along the ducts leading to and from the heater was negligible compared to that along the fluted exhaust-gas passages.

*It should be stated that the pressure drop along the air outlet duct may not be the same when used in the corrugated and noncorrugated units because the heater passages affect the flow conditions at the entrance to the outlet air duct.

Nonisothermal pressure drop.- The nonisothermal static pressure drop of either fluid through the heat exchanger was predicted from isothermal measurements by means of equation (6) of reference 1.

$$\Delta P = \Delta P_{iso} \left(\frac{T_{av}}{T_{iso}}\right)^{1.13} + \left(\frac{G}{3600}\right)^{2} \frac{1}{\gamma_{1g}} \left(\frac{T_2}{T_1} - 1\right) \qquad (14)$$

in which ΔP_{iso} is the total measured isothermal static pressure drop (due to friction alone) at temperature T_{iso}, T_1 and T_2 are the mixed-mean absolute temperatures of the fluid at the inlet and outlet of the heater, respectively, T_{av} is the arithmetic average of T_1 and T_2, G is the fluid rate per unit cross-sectional area and γ_1 is the weight density, evaluated at temperature T_1 of the fluid at the inlet to the heater.

A comparison of measured and predicted nonisothermal pressure drops across each side of the heater is presented in tables V and VI and is shown graphically in figures 8, 9, 12, 13, and 14.

Heat transfer and pressure-drop data for the three heat exchangers are presented in tables I and II.

DISCUSSION

The results of the tests on the three fluted-type heat exchangers are shown graphically. The results obtained for the plain-fluted heater are given in figures 6 to 9 and those for the two corregated fluted heaters (stainless steel and copper) are given in figures 10 to 14.

The corresponding physical dimensions of all three heaters are approximately equal. However, the depth of the ventilating-air passages was slightly less for the corrugated fluted heaters. Also, the stainless steel corrugated fluted heater consisted of sixteen air passages which is the same as the plain fluted heater; whereas, the other corrugated fluted heater, constructed of copper, contained seventeen air passages.

Comparison of Results on Noncorrugated Heater Using Two Different Air Shrouds

The same air shroud was used in all of the tests reported here. A comparison can be made, however, between the present results in the case of the plain fluted heater and those reported for the same heater in reference 1. In the latter experiments a longer air shroud was used which afforded the same cross-sectional area for the flow of ventilating air but had longer inlet and outlet ducts, thus probably yielding a more even distribution of air flow (although an analysis of the measurements of surface temp. near the ends of the heater did not indicate any large difference in the performance in this respect for the two air shrouds). Because the flow areas were equivalent, the rates of heat transfer were about the same for the heater using either shroud (compare fig. 6 of this report to fig. 21 of reference 1). However, the isothermal pressure drop was almost doubled in the case of the air shroud with the shorter inlet and outlet ducts. All of this increase in pressure drop can be ascribed to the greater curvature of the ducts, in which the air is turned in order to flow through the air passages.

Thus, it may be said that if the longer air shroud were also used on the corrugated fluted heaters, the rates of heat transfer would be about the same as for the shorter shroud but the pressure drops would be decreased appreciably. It is undoubtedly true that in many actual installations a limited space would not permit the use of the longer (lower-pressure drop) air shroud.

Heat Transfer

A comparison of the results on the three heaters using the shorter (higher-pressure drop) air shroud reveals that the use of corrugated fluted passages yields thermal conductances approximately 45 percent greater than those obtained with the plain, noncorrugated passages. (Compare figs. 7 and 11.) The rates of heat transfer for the two corrugated fluted heaters were about equal, although the copper heater heat-transfer area was slightly greater due to the additional air passage.

1. Noncorrugated fluted heater.- The predicted overall thermal conductance for the plain fluted heater was

20 to 25 percent lower than the value based upon computations of laboratory measurements. (See fig. 7.) Part of this discrepancy is due to the inability to predict the mechanisms of heat transfer along the tapered ends of the fluted passages. A heat-transfer mechanism equivalent to that along the fully fluted center section of the heater was used along the tapered ends in the prediction calculations. Equations (6) and (7), used in the prediction of (UA) for the plain fluted heater, are based on data taken in smooth ducts where the hydraulic diameter of the passage is used as the significant dimension D. The use of the multiplier (1 + 1.1 D/L) in equations (6) and (7) to account for the higher unit thermal conductance near the entrance of a tube or channel would have yielded magnitudes of (UA) about 7 percent higher than those which were obtained without employing this correction.* (See appendix of reference 9 for a discussion of this correction.)

2. Corrugated fluted heaters.- The predicted overall thermal conductances (UA) for the corrugated fluted heaters agree well (within 10 percent) with the values derived from laboratory measurements. In these calculations the unit thermal conductance (f_c) on either side of the heater was calculated by means of equations (8) and (9), which are based on heat-transfer data from smooth flat plates. The value of the significant dimension l was taken to be the distance between successive crests of the corrugations (i.e., the wave length, $\frac{3}{4}$ in.). This choice is equivalent to stating that a retarded layer is initiated at the crest of each corrugation along the walls of the fluid passages and, therefore, the mechanism of heat transfer is the same as that along successive idealized flat plates. The use of the multiplier (1 + 1.1 D/L) is not necessary for equations (8) and (9), which evaluate the average unit thermal conductance** for the length l. It should also be stated that equations (8) and (9) should be used in regions of systems in which the retarded layer has changed from laminar to turbulent flow. Thus the equations are more applicable for long, flat plates, over which the laminar retarded layer adjacent to the leading edge does not extend along an appreciable portion of the flat plate. The curvature of the corrugated passages in this case probably maintains a turbulent retarded layer rather than a laminar layer.

*Laboratory experiments are now being conducted in order to determine the validity of this correction factor.

**Equations (8) and (9) are used without a correction factor for the D/L effect because the unit thermal conductance is expressed as a function of l.

Isothermal Static Pressure Drop

1. Pressure drops through heater. - The pressure drop along the air side of the corrugated fluted heater was 65 percent greater than that along the air side of the noncorrugated heater. On the exhaust-gas side the corresponding increase was about 130 percent. The fractional increase in pressure drop on the air side was less than that on the gas side because the losses in the air inlet and outlet ducts were about one-half the total loss and were the same on both the corrugated and noncorrugated fluted heaters.

The agreement between the isothermal friction factor ζ_{iso} for the exhaust-gas side of the heater, based on laboratory measurements, and that taken for commercial tubing is excellent. (See fig. 15.) This indicates that the method described above for the calculation of the static pressure drop through the inlet and outlet air ducts; namely, substracting the over-all static pressure drop along the air passages (computed from commercial tube friction factor data) from the total pressure drop across the ducts and the heater, is probably adequate.

If the magnitude of the Reynolds number were the same on both sides of the two corrugated fluted heaters, the magnitude of the friction factor ζ_{iso} for the corrugated passages would be about the same. An inspection of tables III and IV and figure 15 reveals this to be approximately true. The fact that the gas and air passages are not alike in shape, that the passages are tapered at each end, and that all of the wetted perimeter on the air side does not contain corrugations could account for the differences found. A calculation of the isothermal-friction factor from the data of Norris and Snofford (reference 10) for similarly shaped corrugated surfaces revealed a value of $\zeta_{iso} = 0.109$ at a magnitude of Reynolds number of 12,400. At the lowest weight rate used in the tests described in this report (Reynolds number = 10,000) the friction factor was equal to 0.118 for the corner corrugated fluted heater and 0.137 for the stainless-steel heater. The Reynolds number was evaluated by using the hydraulic diameter for the significant dimension D. A similar value of ζ_{iso} was obtained for the sinuous passages on the air side of a cross-flow-type heater described in reference 11.

2. Pressure drop through air ducts.— The complex shape of the inlet and outlet air ducts does not permit a simple prediction of the isothermal pressure drop through these units. In the expression

$$\frac{\Delta P}{\gamma} = K \frac{u_m^2}{2g} \qquad (12)$$

a value of K equal to about 1.0 to 1.5 was found to be appropriate in calculating the duct losses. This magnitude of K is equivalent to that used in computing the pressure drop along a 90° elbow, which the ducts resemble.

Nonisothermal Static-Pressure Drop

The prediction of the nonisothermal static-pressure drop from the measured isothermal pressure drop, by means of equation (14), was successful in all but one instance. (See figs. 8, 9, 12, 13, and 14.)

The slopes of the nonisothermal pressure drop against weight-rate curves are greater than the isothermal curves when the fluid is cooled (gas side) and less when the fluid is heated (air side). An inspection of equation (14) reveals the basis for those facts.

Heater Surface Temperatures

The heater surface temperatures (see tables I and II) appear to be lower for the runs on the stainless-steel heaters than for those on the copper heater. The difficulties encountered in obtaining temperature measurements by the use of thermocouples might account for this deviation.

CONCLUSIONS

1. The thermal performance of the noncorrugated fluted heater can be predicted to within 20 to 25 percent by means of equations (5), (6), and (7), based on heat-transfer data of smooth ducts.

2. The thermal performance of the corrugated fluted heaters can be predicted to within 5 to 10 percent by means of equations (5), (8), and (9), based on heat-transfer data of flat plates, using the wave length of the corrugations as the equivalent flat-plate length.

3. The nonisothermal pressure drop of all the heaters can be adequately predicted from the isothermal pressure drop by means of equation (14).

4. The heaters constructed with corrugated passages instead of plain passages yielded about 45 percent higher rates of heat transfer but increased the pressure drop by about 65 percent on the air side and by about 130 percent on the exhaust-gas side of the heater.

5. The isothermal friction factor along the corrugated passages was two to three times that for the plain passages.

6. The inlet and outlet air ducts accounted for about 83 percent of the total measured isothermal pressure drop in the case of the noncorrugated heater and about 50 percent in the case of the corrugated heater.

7. The heat-transfer rates and pressure drops were approximately equal for the two corrugated fluted heaters (copper and stainless steel).

8. The use of an air shroud with abrupt inlet and outlet ducts on the plain fluted heater yielded the same rates of heat transfer but 100 percent greater pressure drops than did the use of a shroud with longer inlet and outlet ducts.

University of California,
Berkeley, Calif.

REFERENCES

1. Boelter, L. M. K., Miller, M. A., Sharp, W. H., Morrin, E. H., Iversen, H. W. and Mason, W. E.: An Investigation of Aircraft Heaters. IX - Measured and Predicted Performance of Two Exhaust Gas-Air Heat Exchangers and an Apparatus for Evaluating Exhaust Gas-Air Exchangers. NACA A.R.R., March 1943.

2. Martinelli, R. C., Weinberg, E. B., Morrin, E. H., and Boelter, L. M. K.: An Investigation of Aircraft Heaters. III - Measured and Predicted Performance of Double Tube Heat Exchangers. NACA A.R.R., October 1942.

3. Martinelli, R. C., Weinberg, E. B., Morrin, E. H., and Boelter, L. M. K.: An Investigation of Aircraft Heaters. IV - Measured and Predicted Performance of Longitudinally Finned Tubes. NACA A.R.R., October 1942.

4. O'Brien, Morrough P., and Hickox, George, H.: Applied Mechanics. McGraw-Hill Book Co., New York, N.Y., 1937, pp. 211, 350.

5. Committee A-9 Aircraft Air Conditioning Equipment: Airplane Heating and Ventilating Equipment. Engineering Data. SAE Jour., January 1943.

6. Daugherty, R. L.: Hydraulics. A Text on Practical Fluid Mechanics. McGraw-Hill Book Co., New York, N. Y., 1937, p. 226.

7. Gibson, A. H.: Hydraulics and its Application. D. Van Nostrand Co., New York, N. Y., 1925, pp. 251-255.

8. Dodge, Russell A., and Thompson, Milton J.: Fluid Mechanics. McGraw-Hill Book Co., New York, N. Y., 1937, pp. 215-216.

9. Boelter, L. M. K., Dennison, H. G., Guibert, A. G., and Morrin, E. H.: An Investigation of Aircraft Heaters. X - Measured and Predicted Performance of a Fluted-Type Exhaust Gas and Air Heat Exchanger. NACA A.R.R., March 1943.

10. Norris, R. H., and Spofford, W. A. High-Performance Fins for Heat Transfer. Trans. A.S.M.E., vol. 64, no. 5, July 1942, pp. 489-496.

11. Boelter, L. M. K., Dennison, H. G., Guibert, A. G., and Morrin, E. H.: An Investigation of Aircraft Heaters. XII - Performance of a Formed-Plate Crossflow Exhaust-Gas and Air Heat Exchanger. NACA A.R.R., May 1943.

12. Martinelli, R. C., Morrin, E. H., and Boelter, L. M. K.: An Investigation of Aircraft Heaters. VI - Heat Transfer Equations for the Single Pass Longitudinal Exchanger. NACA A.R.R., December 1942.

TABLE I.- EXPERIMENTAL RESULTS ON NON CORRUGATED TYPE HEATER

Run No.	AIR-SIDE						EXHAUST-GAS SIDE						$\frac{q_a}{q_g}$	HEATER TEMPS.		OVERALL PERFORMANCE	
	T_{a_1} °F	T_{a_2} °F	ΔT_a °F	W_a lb/hr	$\Delta P'_a$ Inches H_2O	q_a K.Btu/hr	T_{g_1} °F	T_{g_2} °F	ΔT_g °F	W_g lb/hr	$\Delta P'_g$ Inches H_2O	q_g K.Btu/hr		t_1 °F	t_2 °F	Δt_{lm} °F	(UA) Btu/hr °F
49	98	252	154	4550	20.3	170	1420	1372	48	6670	4.17	88.1	0.52	528	546	1130	150
50	100	297	197	2970	9.88	142	1407	1368	39	6630	4.65	71.1	0.50	644	659	1190	120
51	100	376	276	1610	3.36	108	1428	1390	38	6610	4.52	69.1	0.64	791	834	1170	92.5
54	100	236	136	4700	20.1	155	1415	1355	60	4840	2.54	80.1	0.52	466	504	1220	127
53	102	283	181	3000	9.70	132	1438	1372	66	4840	2.50	87.8	0.67	586	609	1210	109
52	100	353	253	1610	3.31	98.6	1407	1372	35	4850	2.72	46.7	0.47	714	769	1170	84.5
55	99	220	121	4650	20.0	136	1424	1342	82	3590	1.32	81.0	0.60	417	441	1230	111
56	103	264	161	2975	9.30	116	1415	1355	60	3560	1.42	58.8	0.51	526	545	1205	96.5
57	103	331	228	1620	3.30	89.5	1424	1364	60	3560	1.43	58.8	0.66	667	667	1170	76.5

TABLE II.- EXPERIMENTAL RESULTS ON CORRUGATED-FLUTE TYPE HEATER

1. COPPER CONSTRUCTION

	AIR-SIDE						EXHAUST-GAS SIDE							HEATER TEMPS.		OVERALL PERFORMANCE	
Run No.	T_{a_1} °F	T_{a_2} °F	ΔT_a °F	W_a lb/hr	$\Delta P'_a$ Inches H_2O	q_{f_a} K.Btu/hr	T_{g_1} °F	T_{g_2} °F	ΔT_g °F	W_g lb/hr	$\Delta P'_g$ Inches H_2O	q_{f_g} K.Btu/hr	$\frac{q_{f_a}}{q_{f_g}}$	t_1 °F	t_2 °F	Δt_{lm} °F	(UA) Btu/hr°F
9	104	359	255	3700	22.7	228	1424	1321	100	6620	12.1	182	0.80	716	704	1130	202
10	106	426	320	2500	12.1	194	1442	1334	108	6560	11.9	194	1.00	816	819	1110	175
11	111	519	408	1550	5.72	153	1442	1377	65	6520	12.3	99	0.65	929	946	1090	140
14	110	322	212	3800	22.0	195	1429	1300	129	4886	7.20	174	0.89	628	623	1140	171
13	112	383	271	2580	11.5	170	1403	1295	108	4886	6.88	145	0.85	717	720	1090	156
12	110	467	357	1550	5.35	134	1398	1312	86	4886	7.00	116	0.86	835	849	1060	127
15	109	291	182	3850	21.9	170	1411	1265	146	3568	4.15	143	0.84	558	543	1130	150
16	111	357	246	2530	11.4	151	1420	1282	138	3578	4.00	136	0.90	558	662	1110	136
17	112	444	332	1550	5.05	125	1433	1321	112	3568	3.83	110	0.88	786	798	1090	115
2 STAINLESS STEEL CONSTRUCTION																	
26	100	361	261	3400	20.4	215	1414	1316	98	6497	11.8	175	0.81	472	486	1125	191
27	97	399	302	2490	13.0	182	1398	1321	77	6535	11.9	138	0.76	538	555	1100	165
28	99	483	384	1550	5.79	144	1420	1351	69	6446	12.1	122	0.86	671	688	1080	133
29	101	307	206	3470	20.7	174	1416	1278	138	3547	3.80	135	0.78	375	391	1145	151
30	100	356	256	2485	12.0	154	1424	1291	133	3546	3.70	130	0.84	447	462	1115	138
31	104	426	322	1590	5.92	124	1420	1312	108	3496	3.89	104	0.84	555	573	1090	114

TABLE III

NONCORRUGATED FLUTED TYPE HEATER

Isothermal static pressure drop data

W (lb/hr)	G (lb/hr ft²)	ΔP_{iso} (lb/ft²) (a)	= ΔP_{htr} (lb/ft²) (c)	+ ΔP_{ducts} (lb/ft²)	ζ_{iso} (b)	$\zeta_{iso} \frac{L}{D}$ (b)	ζ_{iso} (calculated from data)	Re
			Air side					
1500	13,400	10.9	1.90	9.0	0.033	0.710	------	17,100
2500	22,300	28.5	4.94	23.6	.030	.646	------	28,600
4000	35,700	65.0	11.4	53.6	.028	.604	------	45,500
			Gas side					
4000	20,600	2.23	------	------	0.028	0.329	0.027	45,200
6000	30,900	4.73	------	------	.026	.323	.026	67,800
8000	41,200	8.10	------	------	.024	.298	.025	90,100

[a]Pressure drops obtained from plots of ΔP against W.

[b]ζ_{iso} obtained from fig. 7 of reference 3 (friction factor against Reynolds)

[c]ΔP_{htr} for air side obtained from predicted $(\zeta_{iso}\ L/D)$ (See pg. 12)

$$\frac{\Delta P_{htr}}{\gamma} = \zeta_{iso} \frac{L}{D} \frac{u_m^2}{2g} \qquad (11)$$

TABLE IV

CORRUGATED FLUTED TYPE HEATERS

[Nonisothermal static pressure drop data]

W (lb/hr)	G (lb/hr ft²)	ΔP_{iso} (lb/ft²) (a)	$= \Delta P_{duct}$ (lb/ft²) (b)	$+ \Delta P_{htr}$ (lb/ft²)	ζ_{iso} $\left(\zeta_{iso} \frac{L}{D}\right)$ (calculated from data)		Re
1. Copper Construction							
			Air side				
1500	14,600	17.6	9.00	8.60	0.118	2.62	17,900
2500	24,300	43.1	23.1	20.0	.099	2.20	29,700
4000	39,800	97.7	56.1	41.6	.077	1.71	48,700
			Gas side				
4000	21,400	6.96	-----	-----	0.111	0.989	65,200
6000	32,000	13.9	-----	-----	.099	.883	97,600
8000	42,800	22.6	-----	-----	.090	.802	130,000
2. Stainless-steel construction							
			Air side				
1500	14,400	18.2	9.00	9.20	0.137	2.88	18,600
2500	24,000	46.2	23.1	23.1	.124	2.61	31,000
4000	39,400	109.	56.1	52.9	.111	2.34	50,900
			Gas side				
4000	21,400	6.49	-----	-----	0.0941	0.923	69,000
6000	32,000	12.0	-----	-----	.0778	.762	90,400
8000	42,800	18.6	-----	-----	.0674	.661	138,000

[a]Pressure drops obtained from plots of ΔP against W.

[b]ΔP_{duct} obtained from data on noncorrugated fluted heater (See text, pg. 12.)

TABLE V

NONCORRUGATED FLUTED TYPE HEATER

[Isothermal static pressure drop data]

Run	W (lb/hr)	G (lb/hr ft²)	Measured isothermal pressure drop ΔP_{iso} lb/ft² (T_{iso} = 552 °R) (a)	Measured isothermal pressure drop $\Delta P_{T_{iso}}$ in. H_2O (T_{iso} = 552 °R) (a)	Predicted noniso-thermal pressure drop ΔP lb/ft²	Predicted noniso-thermal pressure drop $\Delta P'$ in. H_2O	Measured noniso-thermal pressure drop ΔP lb/ft²	Measured noniso-thermal pressure drop $\Delta P'$ in. H_2O	T_1 (°R)	T_2 (°R)	T_{av} (°R
Exhaust gas side											
56	3560	18,000	1.81	0.35	5.84	1.12	7.38	1.42	1875	1815	184
53	4840	24,900	3.16	.61	10.1	1.95	13.0	2.50	1898	1832	186
51	6610	34,100	5.66	1.09	19.7	3.80	23.4	4.52	1888	1850	186
Air side											
52	1610	14,400	12.5	2.40	19.1	3.68	17.2	3.31	563	724	64
53	3000	26,800	38.9	7.50	54.0	10.4	50.4	9.70	562	743	65
55	4650	41,500	86.9	16.7	112.	21.6	104.0	20.0	559	680	62

[a]These entries are taken from plot of ΔP_g against W_g or ΔP_a against W_a since actual isothermal measurements were at slightly different fluid rates.

$$\Delta P = \Delta P_{iso} \left(\frac{T_{av}}{T_{iso}}\right)^{1.13} + \left(\frac{G}{3600}\right)^2 \frac{1}{v_1 g}\left(\frac{T_2}{T_1} - 1\right) \qquad (14)$$

$$\Delta P' = \Delta P \times \frac{12}{62.3} \text{ in. } H_2O$$

TABLE VI

CORRUGATED FLUTED HEATER

[Nonisothermal static pressure drop data]

Run	W (lb/hr)	G (lb/hr ft^2)	Measured isothermal pressure drop ΔP_{iso} lb/ft^2	Measured isothermal pressure drop $\Delta P'_{iso}$ in. H_2O	Predicted nonisothermal pressure drop ΔP lb/ft^2	Predicted nonisothermal pressure drop $\Delta P'$ in. H_2O	Measured nonisothermal pressure drop ΔP lb/ft^2	Measured nonisothermal pressure drop $\Delta P'$ in. H_2O	T_1 (°R)	T_2 (°R)	T_{av} (°R)
1. Copper heater											
Exhaust gas side											
16	3580	19,100	6.00	1.16	21.9	4.23	20.8	4.00	1902	1837	1870
12	4890	26,100	10.2	1.96	34.4	6.64	36.3	7.00	1902	1794	1848
9	6620	35,400	16.6	3.20	55.7	10.8	62.8	12.1	1884	1781	1833
Air side											
12	1550	15,100	18.5	3.57	29.9	5.76	27.8	5.35	570	927	749
16	2530	24,500	44.0	8.50	63.1	12.2	58.9	11.4	571	817	694
14	3800	36,900	90.0	17.4	125.7	24.2	114.0	22.0	570	782	676
2. Stainless steel heater											
Exhaust gas side											
31	3500	18,700	5.10	0.98	17.5	3.38	20.2	3.89	1880	1772	1826
27	6540	34,900	13.5	2.60	46.3	9.00	61.7	11.9	1858	1781	1820
Air side											
28	1550	14,900	19.5	3.76	32.1	6.20	30.0	5.79	559	943	751
27	2490	24,000	45.0	8.68	68.9	13.3	67.2	13.0	557	859	708
26	3400	32,700	78.0	15.0	115.8	22.3	105.6	20.4	560	821	690

[a]The entries are taken from plot of ΔP_g against W_g or ΔP_a against W_a, since actual isothermal measurements are at slightly different fluid rates.

$$\Delta P = \Delta P_{iso}\left(\frac{T_{av}}{T_{iso}}\right)^{1.13} + \left(\frac{G}{3600}\right)^2 \frac{1}{\gamma_{1g}}\left(\frac{T_2}{T_1} - 1\right) \qquad (14)$$

$$\Delta P' = \Delta P \times \frac{12}{62.3} \text{ in. } H_2O$$

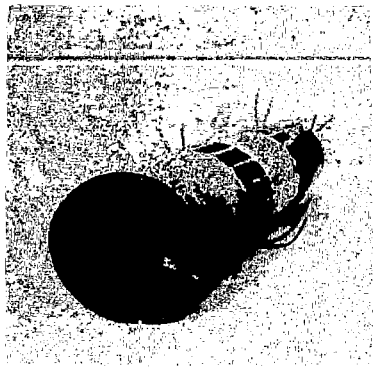

Figure 1.- Photograph of corrugated-flute type heater (stainless steel).

Figure 2.- Photograph of corrugated-flute type heater (copper).

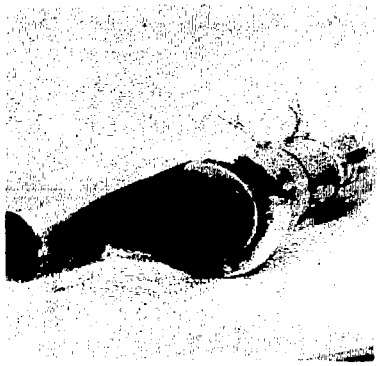

Figure 3.- Photograph of air shroud used on flute-type heaters.

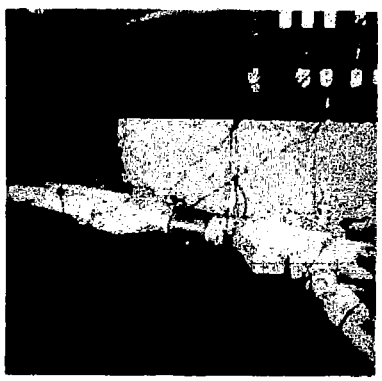

Figures 4 and 5 - Photograph of heaters in test stand.

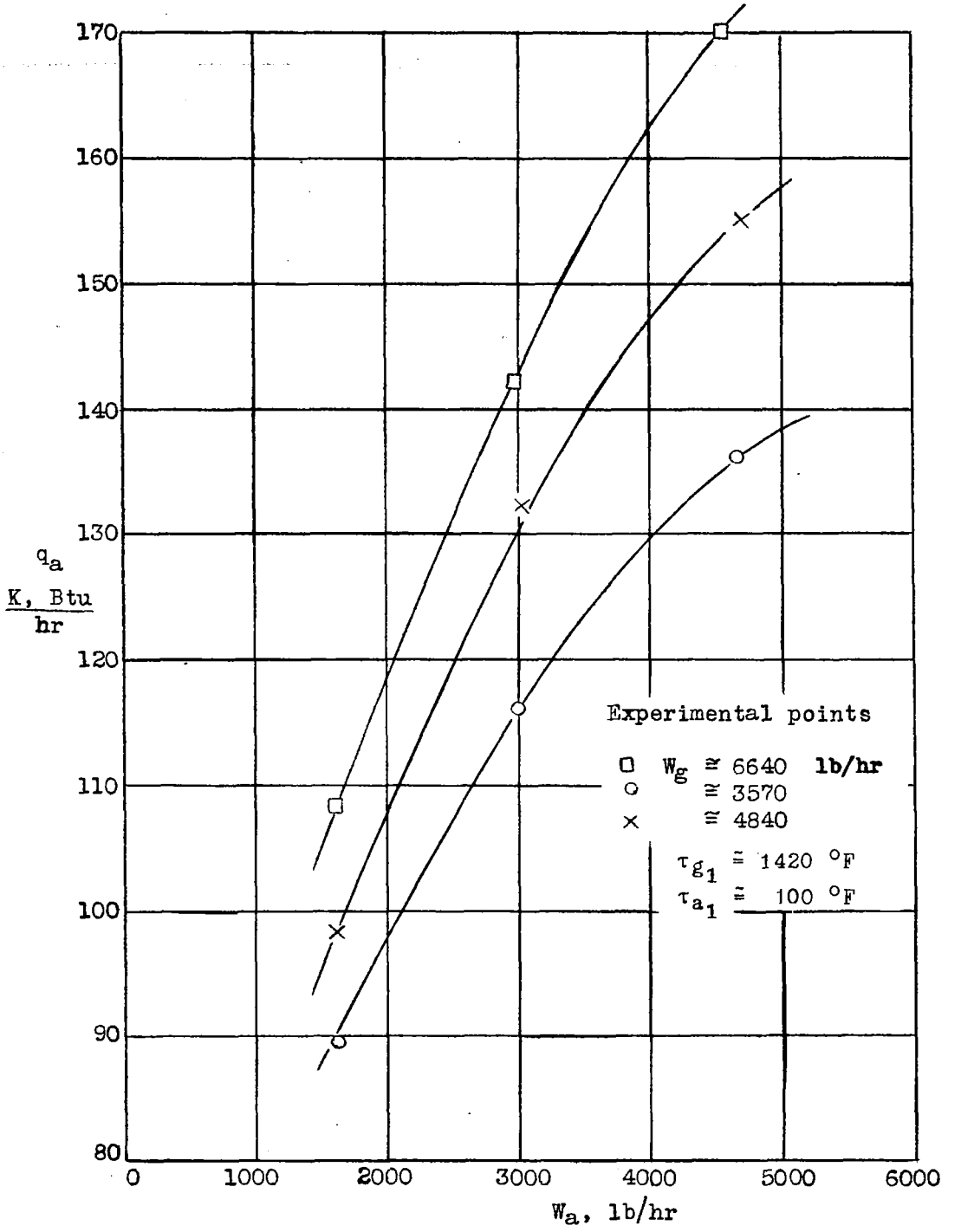

Figure 6.- Thermal output of non-corrugated flute type heater as a function of ventilating-air rate.

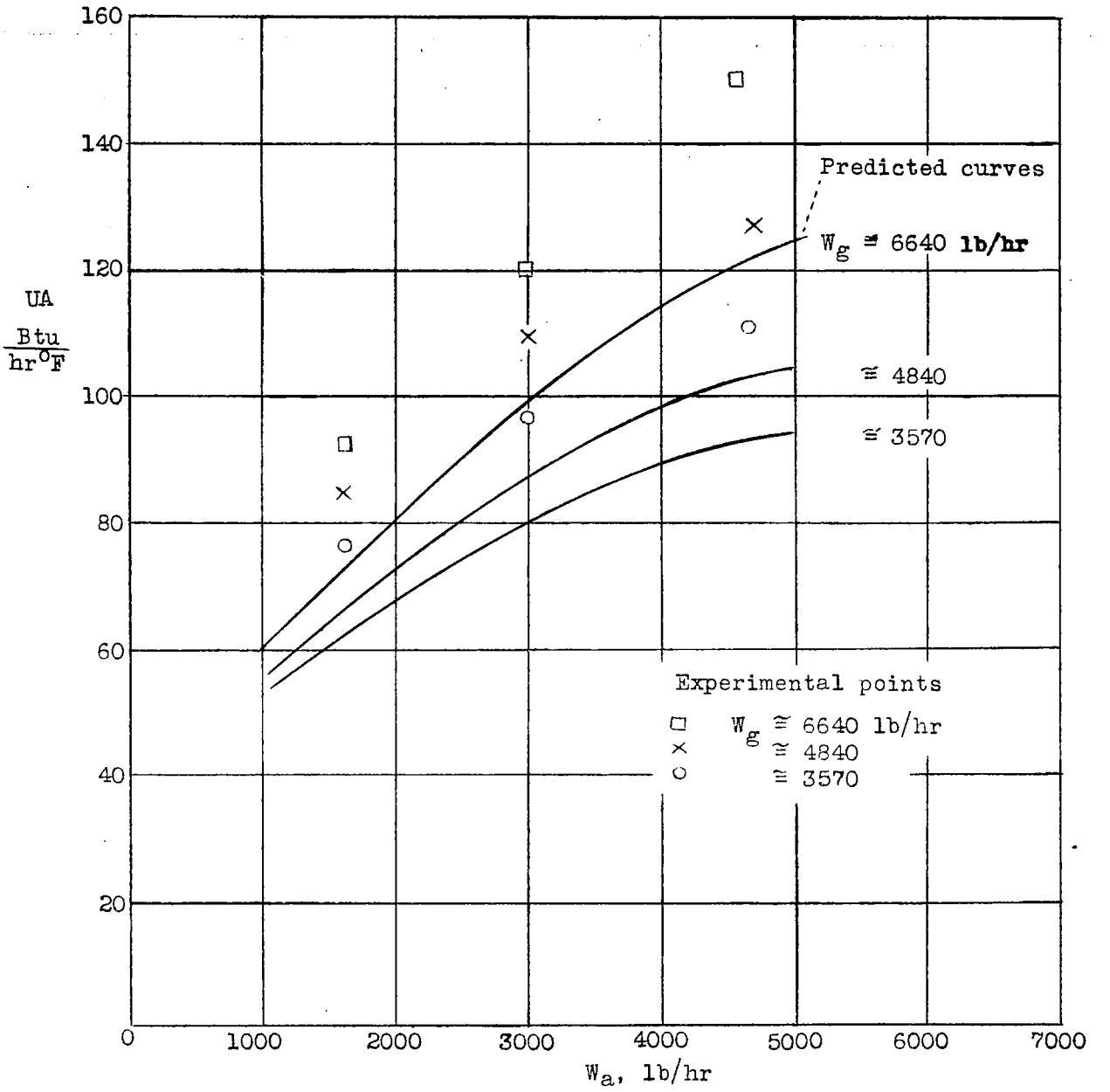

Figure 7. - Over-all thermal conductance of non-corrugated flute type heater as a function of ventilating-air rate.

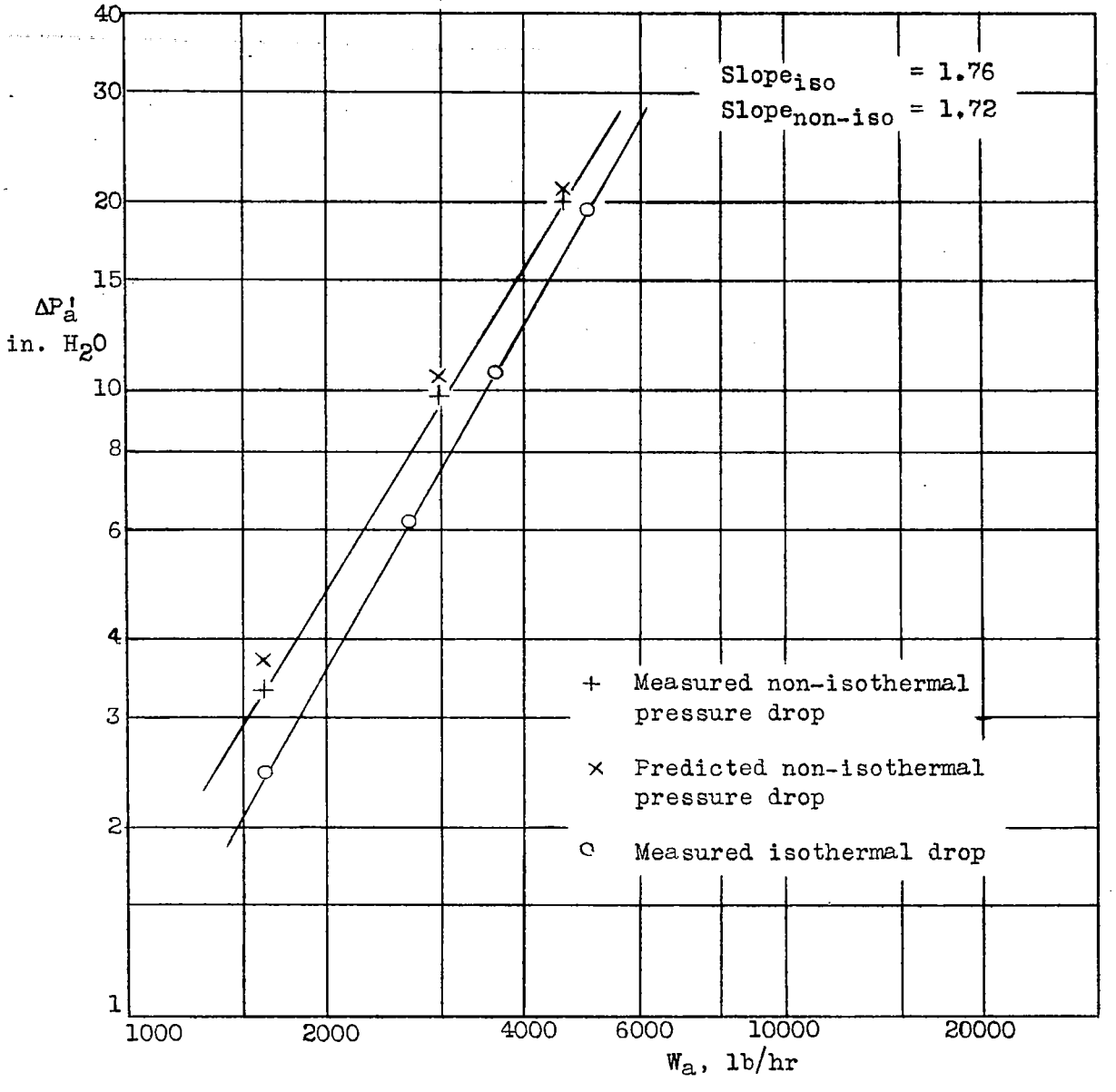

Figure 8.- Static pressure drop on air side of non-corrugated flute type heater as a function of ventilating-air rate.

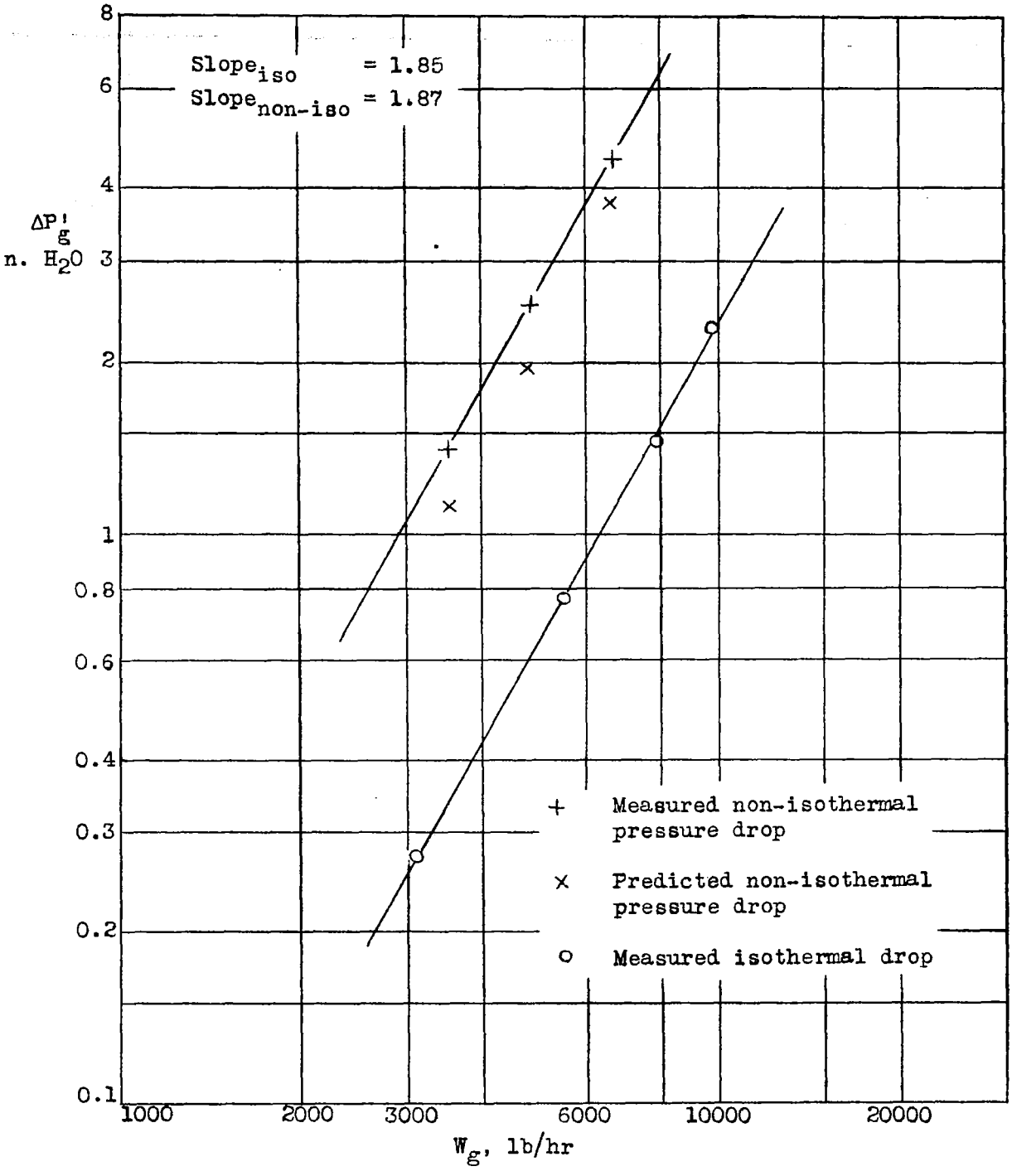

Figure 9.- Static pressure drop on the gas side of a non-corrugated flute type heater as a function of the exhaust-gas rate.

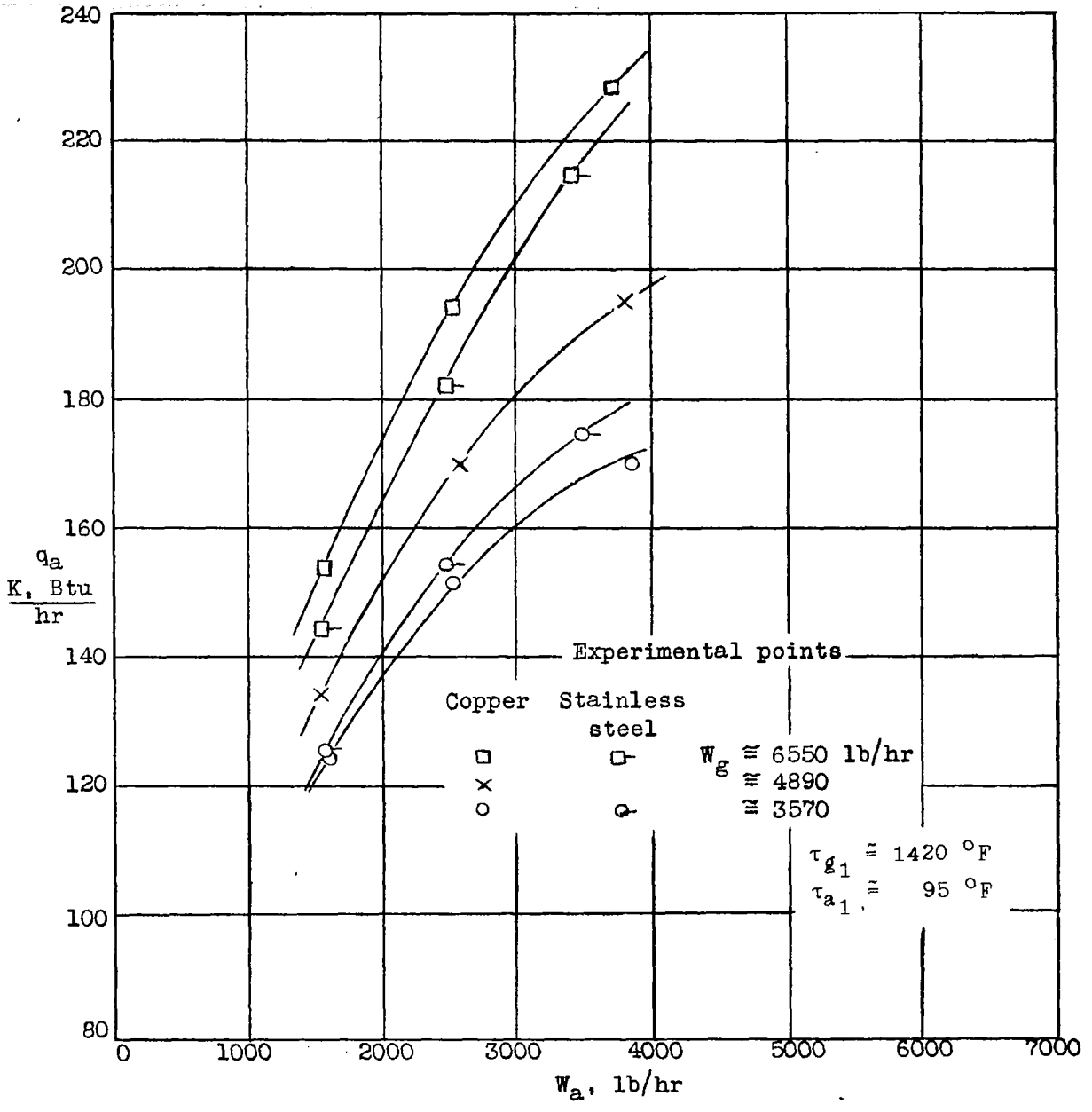

Figure 10.- Thermal output of corrugated-flute type heater as a function of ventilating-air rate.

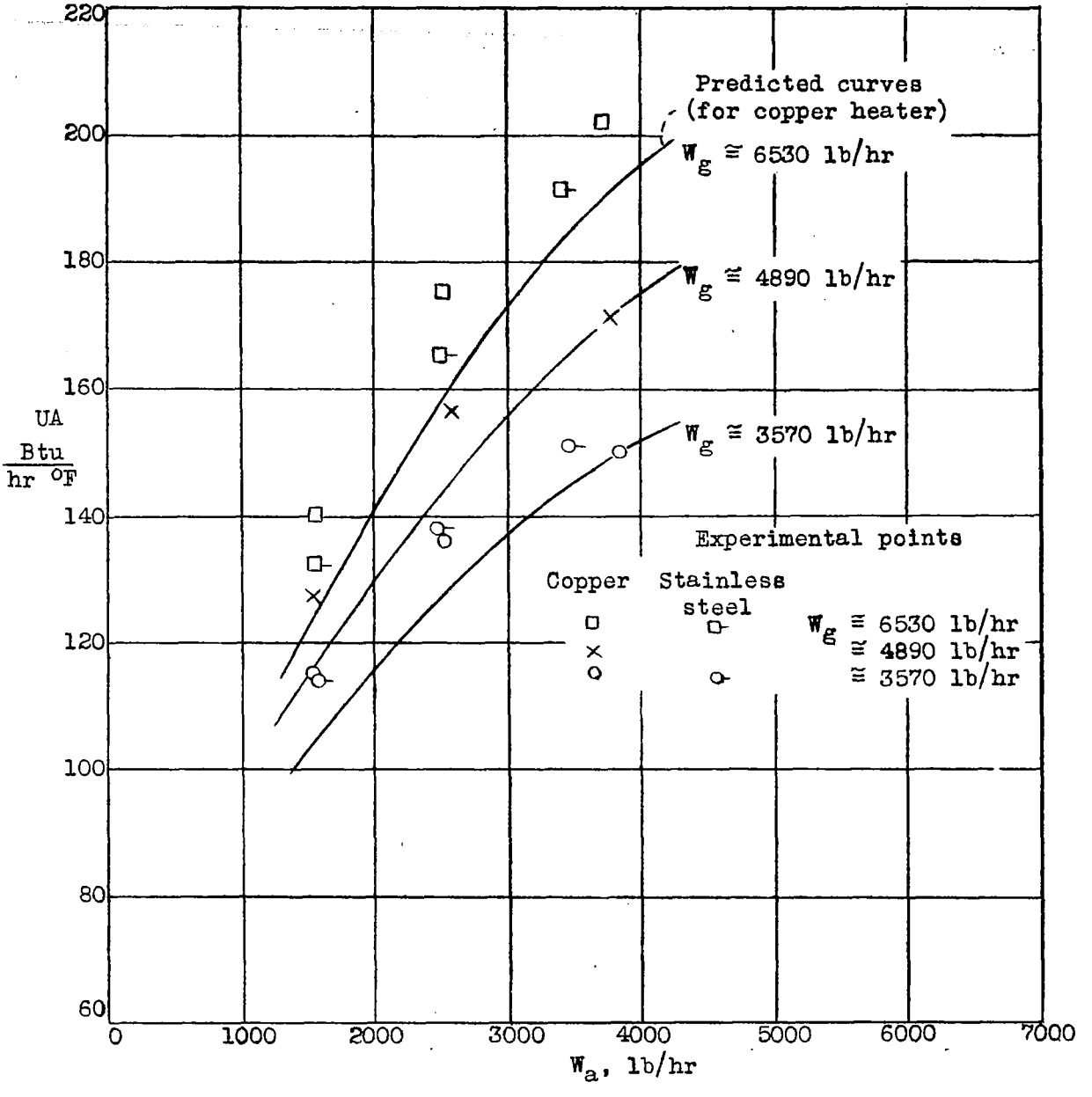

Figure 11.- Over-all conductance of corrugated-flute type heater as a function of ventilating-air rate.

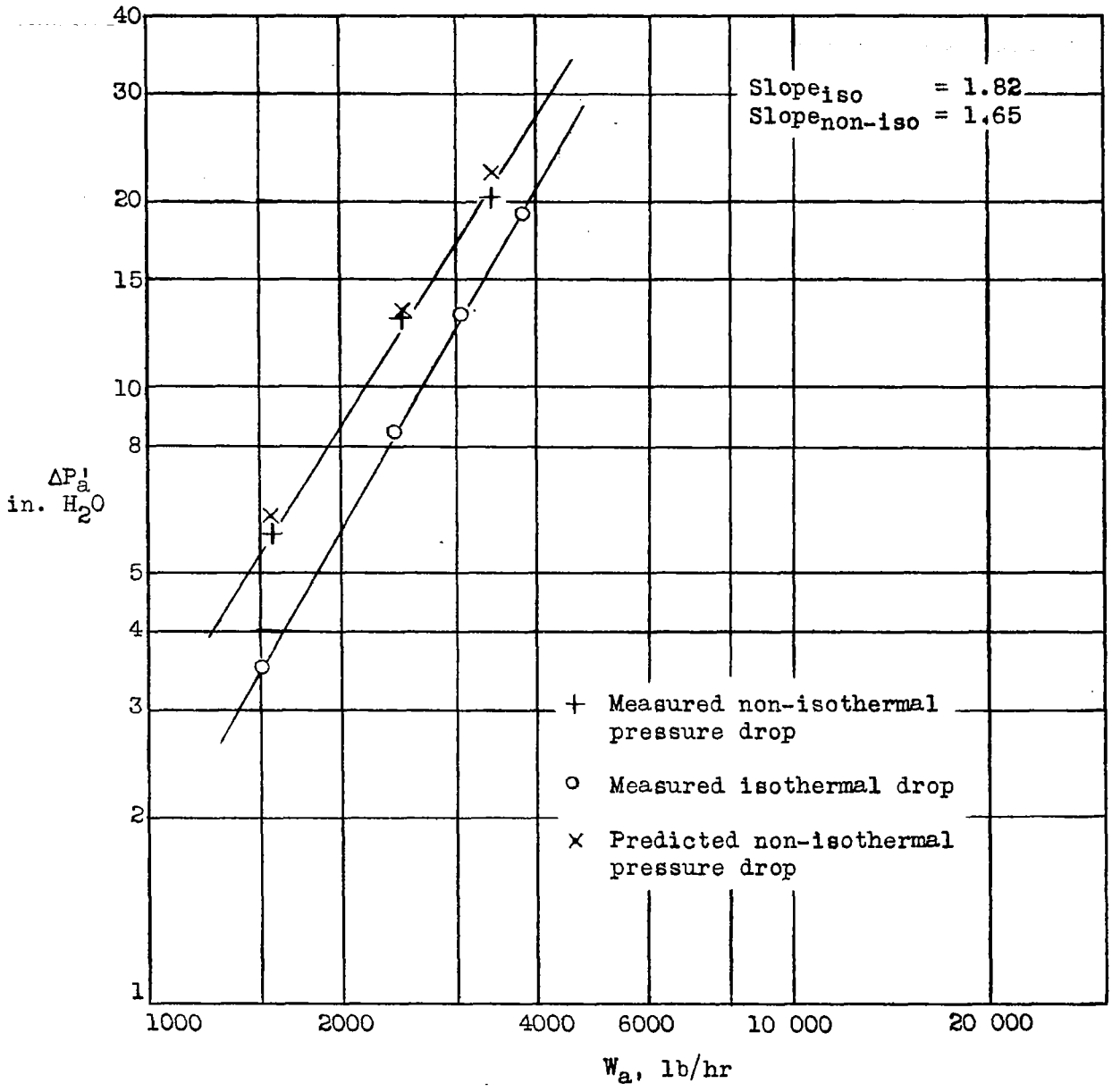

Figure 12.- Static pressure drop on ventilating-air side of a corrugated-flute type heater (stainless steel) as a function of ventilating-air rate.

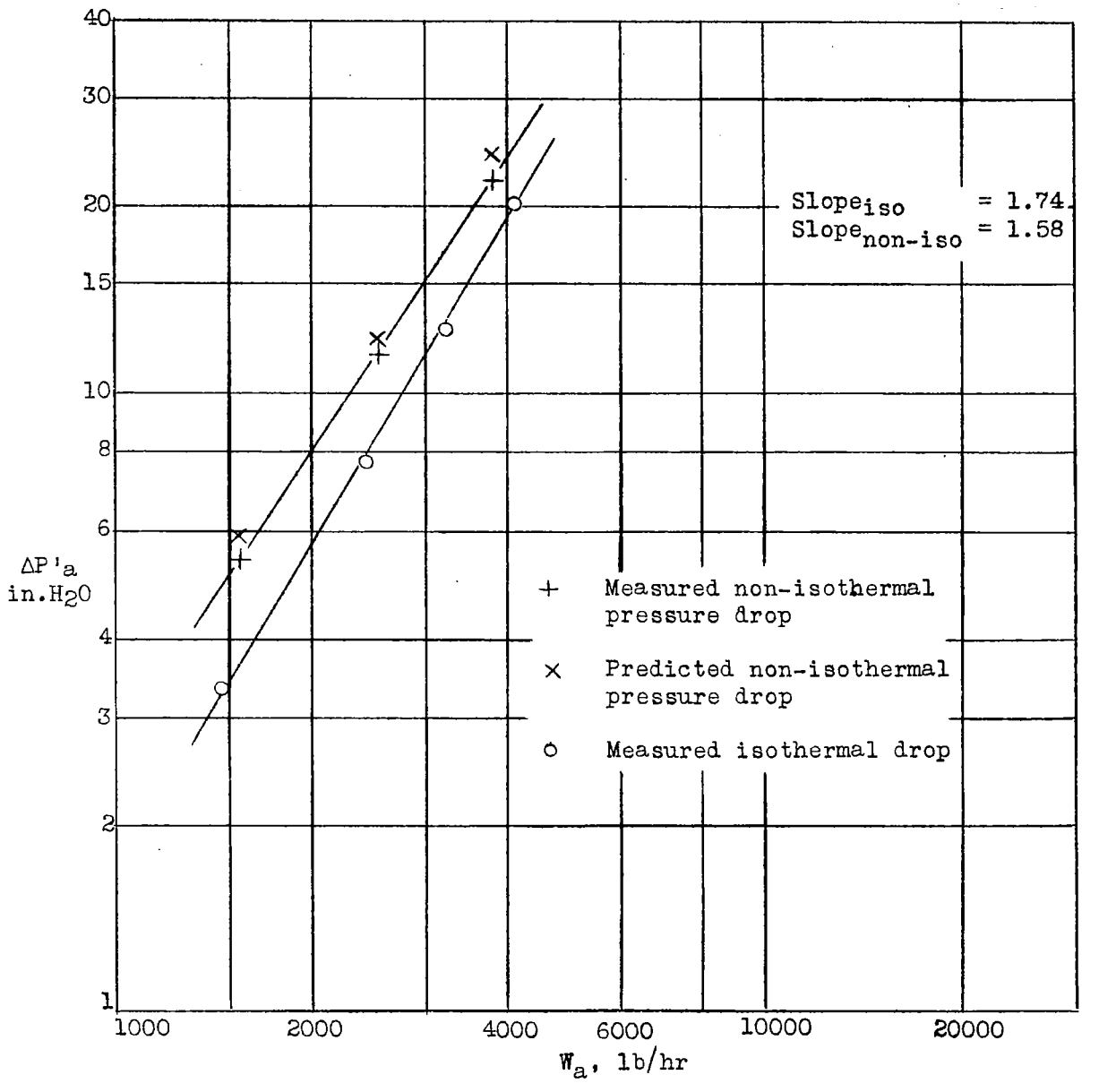

Figure 13.- Static pressure drop on ventilating-air side of corrugated-flute type (copper) heater as a function of ventilating-air rate.

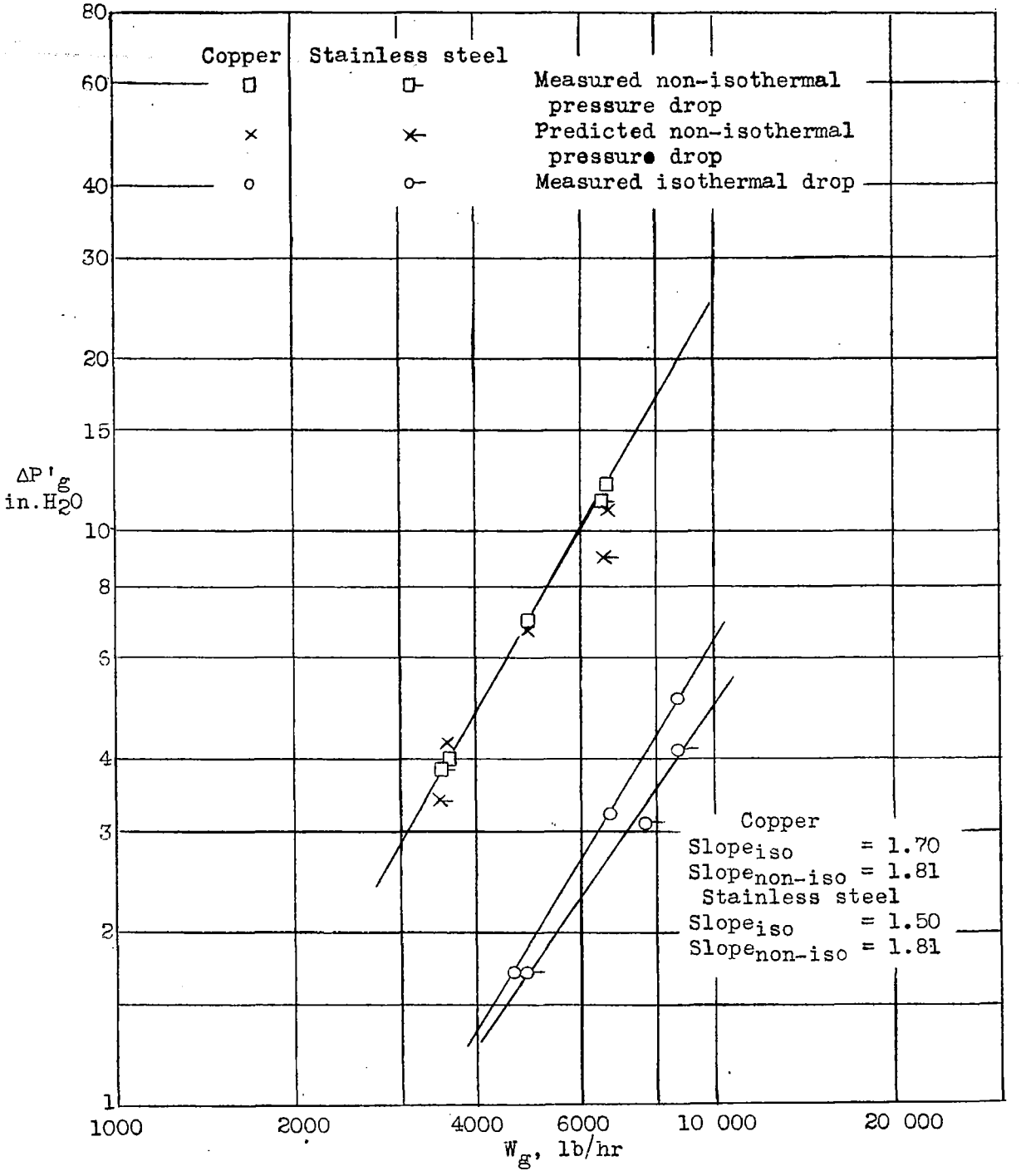

Figure 14.- Static pressure drop on exhaust-gas side of corrugated-flute type heater (copper and stainless steel) as a function of exhaust-gas rate.

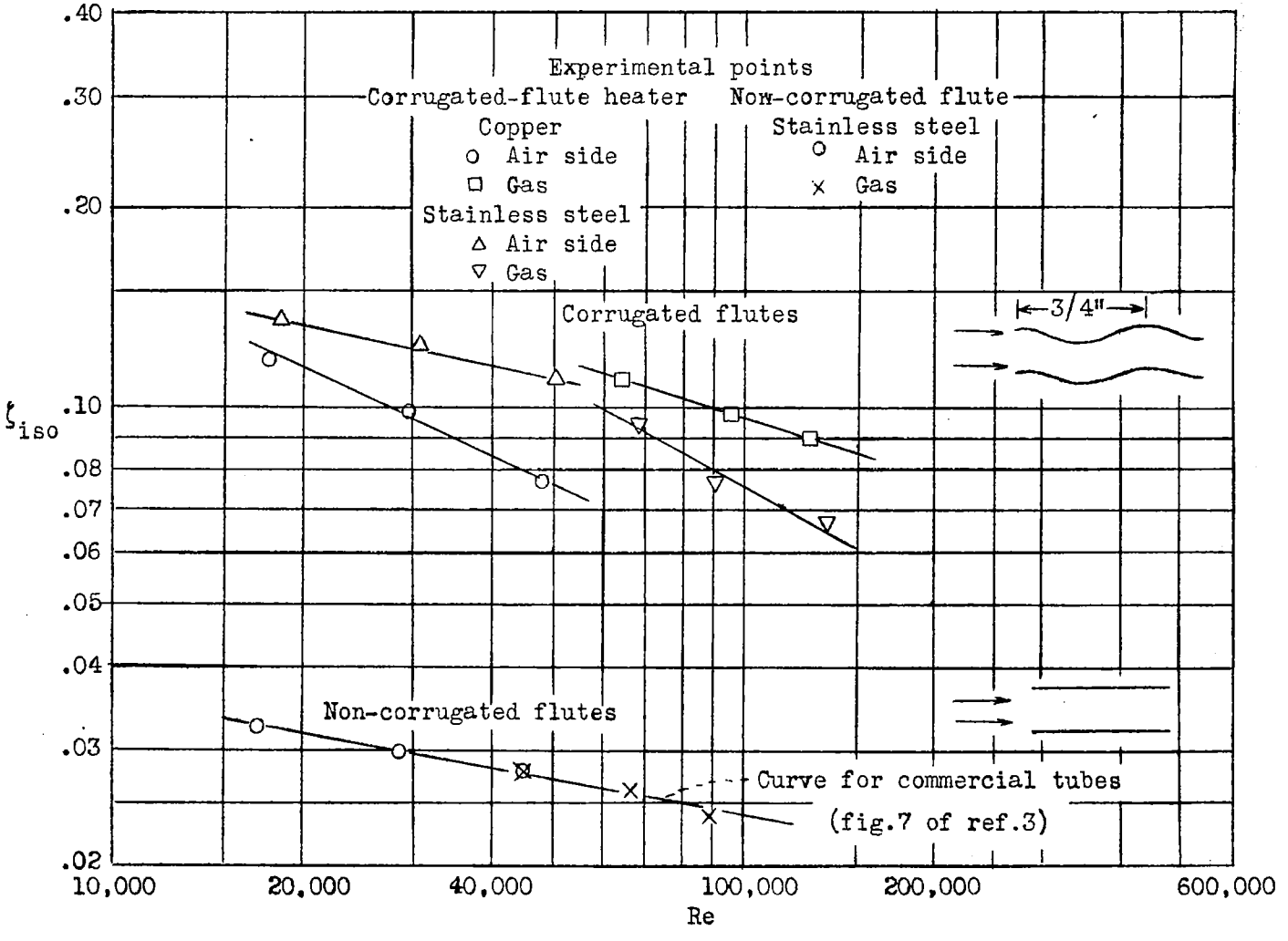

Figure 15.- Isothermal friction factor as a function of Reynolds number.

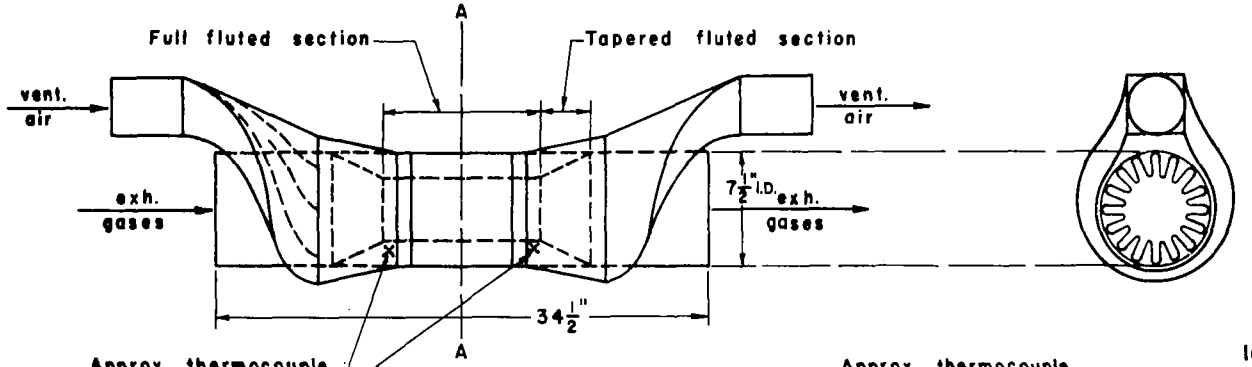

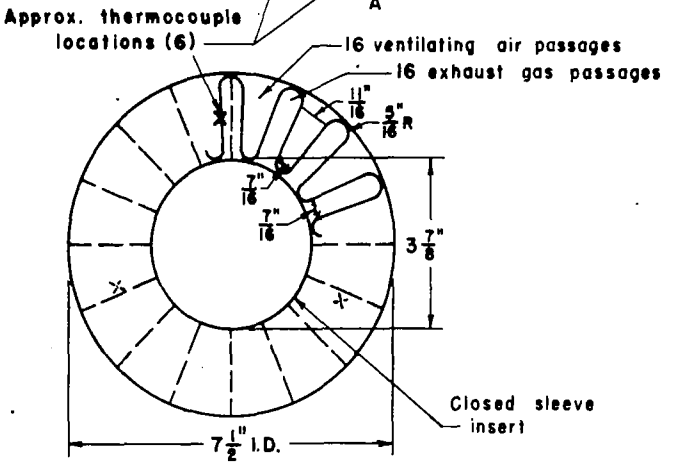

Section A-A

Plain fluted type
(Stainless steel)

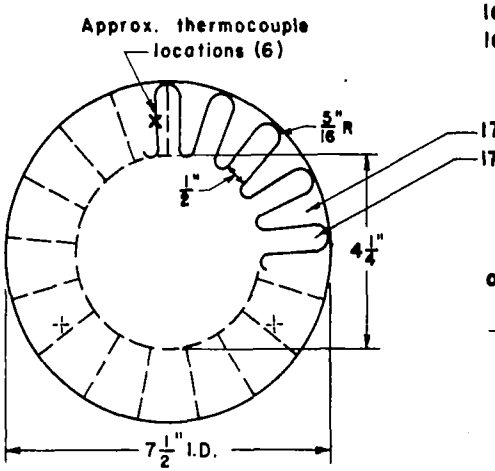

Section A-A

Corrugated fluted type
(Copper)

(Stainless steel heater)
16 ventilating air passages
16 exhaust gas passages

(Copper heater)
17 ventilating air passages
17 exhaust gas passages

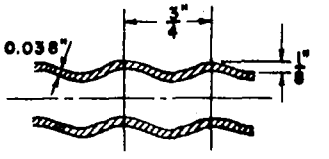

Corrugated section

	Plain (stainless steel)		Corrugated (copper)		Corrugated (stainless steel)	
	Air	Gas	Air	Gas	Air	Gas
Cross section area, ft.² (At section A-A)	0.112	0.194	0.103	0.187	0.104	0.187
Wetted perimeter, ft. (" " ")	7.60	7.68	7.28	5.32	6.97	5.01
Heat transfer area, ft.²	7.19	7.19	6.92	6.92	6.50	6.50
Length of full fluted section, ft.	0.917	0.917	0.958	0.958	0.958	0.958
Length of each tapered fluted section, ft.	0.354	0.354	0.292	0.292	0.292	0.292
Wt. of heater, lb.	19½		24¾		18	
Wt. of shroud, (8½ lb.)						

Fig. 16.- Schematic Diagram of Solar Heaters and Air Shroud.

NACA

Fig. 16